Available online at www.sciencedirect.com
SCIENCE DIRECT®
C. R. Physique 5 (2004) 9–20
COMPTES RENDUS PHYSIQUE

Bose–Einstein condensates: recent advances in collective effects/Avancées récentes sur les effets collectifs dans les condensats de Bose–Einstein

Properties of vortices in Bose–Einstein condensates

Amandine Aftalion

Laboratoire Jacques-Louis Lions, Université Paris 6, 175, rue du Chevaleret, 75013 Paris, France

Presented by Guy Laval

Abstract

One of the key issues related to superfluidity is the existence of quantized vortices. Following recent experiments on Bose–Einstein condensates exhibiting vortices, we investigate the behavior of the wave function which solves the Gross–Pitaevskii equation. For a rotating Bose–Einstein condensate in a harmonic trap, we give a simplified expression of the Gross–Pitaevskii energy in the Thomas–Fermi regime, which only depends on the number and shape of the vortex lines. This allows us to study in detail the structure of the line of a single quantized vortex, which has a U or S shape. S type vortices exist for all values of the angular velocity Ω but are not minimizers of the energy while U vortices are minimizers and exist only for Ω sufficiently large. Finally, we study the drag created by the movement of a detuned laser beam in a condensate and the nucleation of vortices in the low density region close to the boundary layer of the cloud. ***To cite this article: A. Aftalion, C. R. Physique 5 (2004).***

Résumé

Propriétés des vortex pour des condensats de Bose Einstein. Une des questions reliées à la superfluidité est l'existence de vortex quantifiés. Suite aux récentes expériences dans les condensats de Bose Einstein mettant en évidence des vortex, nous étudions les propriétés de la fonction d'onde qui est solution d'une équation de Gross Pitaevskii. Pour un condensat en rotation dans un piège harmonique, nous donnons une expression simplifiée de l'énergie de Gross Pitaevskii dans la limite de Thomas–Fermi, qui ne dépend que du nombre et de la forme des lignes de vortex. Cela nous permet d'étudier la structure des lignes de vortex, qui sont du type U ou S. Les vortex de type S existent pour toute valeur de la vitesse de rotation Ω mais ne sont pas minimiseurs de l'énergie, tandis que les U n'existent que pour Ω plus grand qu'une valeur critique et sont alors minimiseurs. Enfin, nous étudions la traînée engendrée par le déplacement d'un laser dans un condensat et la nucléation des vortex dans la zone de basse densité. ***Pour citer cet article : A. Aftalion, C. R. Physique 5 (2004).***

Keywords: Bose–Einstein condensates; Vortices

Mots-clés : Condensats de Bose Einstein ; Vortex

1. Introduction

Since the first experimental achievement of Bose–Einstein condensation in confined alkali gases in 1995, many properties of these systems have been studied experimentally and theoretically [1–10]. One of the key issues, related to superfluidity, is the existence of vortices. In that respect, there are two classical experiments to obtain quantized vortices. One consists in stirring a laser beam along the condensate in a translation movement [11–13]: this is the equivalent of moving an object in a superfluid, so that there is a critical velocity below which the movement is dissipationless and beyond which the stirring produces vortices. On the other hand, there is also the classical rotating bucket experiment: a consequence of superfluidity is the existence of

E-mail address: amandine.aftalion@math.jussieu.fr (A. Aftalion).

1631-0705/$ – see front matter
doi:10.1016/j.crhy.2004.01.001

permanent currents. Several experimental groups have produced vortices by a rotation of the trapping potential, in particular the group of Dalibard at the ENS in Paris [7,8,14] and the group of Ketterle at MIT [15,16]. In the ENS experiment, a laser beam is imposed on the magnetic trap holding the atoms to create a harmonic anisotropic rotating potential. For small angular velocities, no modification of the condensate is observed. For sufficiently large angular velocities, vortices are detected in the system. The particularity of the vortex line is that it is not straight along the axis of rotation but bending. Numerical computations solving the Gross–Pitaevskii equation [17,18] have shown that there is a range of velocities for which the vortex line is indeed bending. The aim of this paper is to justify these observations theoretically in the Thomas–Fermi regime and study in detail theoretically and numerically the shape of the vortex lines. We define an asymptotic parameter which is small in the Thomas–Fermi regime and approximate the Gross–Pitaevskii energy to obtain a simpler form of the energy which only depends on the shape of the vortex lines. Then we check that our characterization leads to solutions with a bent vortex for a range of values of the rotational velocity which are consistent with the ones observed.

The Gross–Pitaevskii energy provides a very good description of Bose–Einstein condensates: it is assumed that the N particles of the gas are condensed in the same state described by the wave function ϕ. By introducing a rotating frame at angular velocity $\widetilde{\Omega} = \widetilde{\Omega}\mathbf{e}_z$, the trapping potential becomes time independent, and the wave function ϕ minimizes the energy

$$\mathcal{E}_{3D}(\phi) = \int \frac{\hbar^2}{2m}|\nabla\phi|^2 + \hbar\widetilde{\Omega}\cdot(\mathrm{i}\phi, \nabla\phi\times\mathbf{x}) + \frac{m}{2}\sum_{\alpha}\omega_\alpha^2 r_\alpha^2|\phi|^2 + \frac{N}{2}g_{3D}|\phi|^4, \tag{1}$$

under the constraint $\int|\phi|^2 = 1$. Here, for any complex quantities u and v and their complex conjugates $\bar{u}$ and $\bar{v}$, $(u,v) = (u\bar{v}+\bar{u}v)/2$ and $g_{3D} = 4\pi\hbar^2 a/m$. We want to nondimensionalize the energy in order to get a parameter which is small in the Thomas–Fermi regime. We define the characteristic length $d = (\hbar/m\omega_x)^{1/2}$ and assume $\omega_y = \alpha\omega_x$, $\omega_z = \beta\omega_x$. We set

$$\varepsilon = \left(\frac{d}{8\pi Na}\right)^{2/5}. \tag{2}$$

For numerical applications, we are going to use the experimental values of the ENS group [8], $m = 1.445\times10^{-25}$ kg, $a = 5.8\times10^{-11}$ m, $N = 1.4\times10^5$ and $\omega_x = 1094\ \mathrm{s}^{-1}$ with $\alpha = 1.06$, $\beta = 0.067$. We find that $\varepsilon = 0.0174$, thus, ε is small, which will be our asymptotic regime. We re-scale the distance by $R = d/\sqrt{\varepsilon}$ and define $u(\mathbf{r}) = R^{3/2}\phi(\mathbf{x})$ where $\mathbf{x} = R\mathbf{r}$ and we set $\Omega = \widetilde{\Omega}/\varepsilon\omega_x$. The velocity Ω is chosen such that $\Omega < 1/\varepsilon$, that is the trapping potential is stronger than the inertial potential. The energy can be rewritten as:

$$E_{3D}(u) = \int \frac{1}{2}|\nabla u|^2 + \Omega\cdot(\mathrm{i}u, \nabla u\times\mathbf{r}) + \frac{1}{2\varepsilon^2}\left(x^2+\alpha^2y^2+\beta^2z^2\right)|u|^2 + \frac{1}{4\varepsilon^2}|u|^4. \tag{3}$$

Due to the constraint $\int|u|^2 = 1$, we can add to E_{3D} any multiple of $\int|u|^2$ so that it is equivalent to minimize

$$E_\varepsilon(u) = \int \frac{1}{2}|\nabla u|^2 + \Omega\cdot(\mathrm{i}u, \nabla u\times\mathbf{r}) + \frac{1}{4\varepsilon^2}|u|^4 - \frac{1}{2\varepsilon^2}\rho_{\mathrm{TF}}(\mathbf{r})|u|^2, \tag{4}$$

where $\rho_{\mathrm{TF}}(\mathbf{r}) = \rho_0 - (x^2+\alpha^2y^2+\beta^2z^2)$ is the Thomas–Fermi approximation of u, and ρ_0 is determined by

$$\int_{\mathcal{D}} \rho_{\mathrm{TF}}(\mathbf{r}) = 1. \tag{5}$$

$\mathcal{D}$ is the ellipsoid $\{\rho_{\mathrm{TF}} > 0\} = \{x^2+\alpha^2y^2+\beta^2z^2 < \rho_0\}$, which yields $\rho_0^{5/2} = 15\alpha\beta/8\pi$. To study the problem analytically, it is reasonable to minimize the energy E_ε over the domain $\mathcal{D}$ with zero boundary data for u. Indeed, when $\rho_{\mathrm{TF}} \leqslant 0$, the energy is convex so that the minimizer u goes to zero exponentially quickly away from the condensate (see the numerical observation in [6]). In fact the boundary layer where ρ_{TF} is matched to zero, is of size $\varepsilon^{2/3}$ and the behaviour of the wave function in the layer is given by a Painlevé equation (for the analysis on the behaviour near the boundary of $\mathcal{D}$ as well as the decay at infinity of the order parameter, see [19,20]).

Note that a critical point u of E_ε is a solution of

$$-\Delta u + 2\mathrm{i}(\Omega\times\mathbf{r})\cdot\nabla u = \frac{1}{\varepsilon^2}u\left(\rho_{\mathrm{TF}} - |u|^2\right) + \mu_\varepsilon u \quad \text{in } \mathcal{D}, \tag{6}$$

with $u = 0$ on $\partial\mathcal{D}$ and μ_ε is the Lagrange multiplier. The specific choice of ρ_0 will imply that the term $\mu_\varepsilon u$ is negligible in front of $\rho_{\mathrm{TF}}u/\varepsilon^2$.

We have set the framework of study of the energy E_ε. We will make an asymptotic expansion of the energy taking into account that ε is small. The aim is to reach a simplified expression of the energy depending on the vortex lines. Then we will study the shape of a single vortex line in the light of the recent experiments [14]. We also show numerical simulations of the full Gross–Pitaevskii equations. Finally, we describe results concerning the nucleation of vortices in the Painlevé boundary layer of a condensate. All the results presented here are contained in [21–25].

2. Asymptotic expansion of the energy

Our aim is to decouple the energy E_ε into 3 terms: a part coming from the profile of the solution without vortices, a vortex contribution and a term due to rotation. The analysis described in this section relies on [22].

2.1. The solution without vortices

Firstly, we are interested in the profile of solutions so that we will study solutions without vortices. Thus we consider functions of the form $\eta = f\,\mathrm{e}^{\mathrm{i}S}$, f is real and does not vanish in the interior of $\mathcal{D}$. We first minimize E_ε over such functions without imposing the constraint that the norm is 1. When ε is small, since the ellipticity of the cross-section is small, the zero order approximation of f_ε^2 is ρ_{TF}. As for the phase, its behaviour is given by the continuity equation $\operatorname{div}(f_\varepsilon^2(\nabla S_\varepsilon - \Omega \times \mathbf{r})) = 0$. This implies that there exists Ξ_ε such that

$$f_\varepsilon^2(\nabla S_\varepsilon - \Omega \times \mathbf{r}) = \Omega \operatorname{curl} \Xi_\varepsilon. \tag{7}$$

One can think of Ξ_ε as the equivalent of a stream function in the case of fluid vortices. Ξ_ε is the solution of

$$\operatorname{curl}\left(\frac{1}{f_\varepsilon^2}\operatorname{curl}\Xi_\varepsilon\right) = -2 \quad \text{in } \mathcal{D}, \qquad \Xi_\varepsilon = 0 \quad \text{on } \partial\mathcal{D}. \tag{8}$$

When ε is small, the function Ξ_ε is well approximated by the solution Ξ of

$$\operatorname{curl}\left(\frac{1}{\rho_{\mathrm{TF}}}\operatorname{curl}\Xi\right) = -2 \quad \text{in } \mathcal{D}, \qquad \Xi = 0 \quad \text{on } \partial\mathcal{D}. \tag{9}$$

One can easily get that $\Xi(x,y) = -\rho_{\mathrm{TF}}^2(x,y)/(2+2\alpha^2)\mathbf{e}_z$. Using (7), we can define S_0, the limit of S_ε, to be the solution of $\rho_{\mathrm{TF}}(\nabla S_0 - \Omega \times \mathbf{r}) = \Omega \operatorname{curl} \Xi$ with zero value at the origin. We have $S_0 = C\Omega xy$ with $C = (\alpha^2-1)/(\alpha^2+1)$. We see that S_0 vanishes when $\alpha = 1$ that is when the cross-section is a disc. This computation is consistent with the one in [9], though it is derived in a different way. The function $\eta_\varepsilon = f_\varepsilon\,\mathrm{e}^{\mathrm{i}S_\varepsilon}$ that we have studied gives the profile of any solution. It will allow us to compute the energy of all solutions.

2.2. Decoupling the energy

Let $\eta_\varepsilon = f_\varepsilon\,\mathrm{e}^{\mathrm{i}S_\varepsilon}$ be the vortex free minimizer of E_ε discussed above. Let u_ε be a configuration that minimizes E_ε and let $v_\varepsilon = u_\varepsilon/\eta_\varepsilon$. Since η_ε satisfies the Gross–Pitaevskii equation (6) with $\mu_\varepsilon = 0$, we have

$$\int_{\mathcal{D}} \left(|v_\varepsilon|^2 - 1\right)\left(-\frac{1}{2}\Delta f_\varepsilon^2 - \frac{1}{\varepsilon^2} f_\varepsilon^2\left(\rho_{\mathrm{TF}} - f_\varepsilon^2\right) + \left|\nabla f_\varepsilon\,\mathrm{e}^{\mathrm{i}S_\varepsilon}\right|^2 - 2f_\varepsilon^2(\nabla S_\varepsilon \cdot \Omega \times \mathbf{r})\right) = 0. \tag{10}$$

This trick was introduced in [27] and leads to the following exact decoupling of the energy $E_\varepsilon(u_\varepsilon)$:

$$E_\varepsilon(u_\varepsilon) = E_\varepsilon(\eta_\varepsilon) + G_{\eta_\varepsilon}(v_\varepsilon) + I_{\eta_\varepsilon}(v_\varepsilon), \tag{11}$$

where

$$G_{\eta_\varepsilon}(v_\varepsilon) = \int_{\mathcal{D}} \frac{1}{2}|\eta_\varepsilon|^2|\nabla v_\varepsilon|^2 + \frac{|\eta_\varepsilon|^4}{4\varepsilon^2}\left(1 - |v_\varepsilon|^2\right)^2,$$

is the energy of vortices and

$$I_{\eta_\varepsilon}(v_\varepsilon) = \int_{\mathcal{D}} |\eta_\varepsilon|^2(\nabla S_\varepsilon - \Omega \times \mathbf{r}) \cdot (\mathrm{i}v_\varepsilon, \nabla v_\varepsilon),$$

is the angular momentum of vortices. The first term $E_\varepsilon(\eta_\varepsilon)$ is independent of the solution u_ε, so we have to compute the next two and find for which configuration u_ε the minimum is achieved. We use that at zero order $|\eta_\varepsilon|^2 = f_\varepsilon^2$ is approximated by ρ_{TF} when ε is small so that we can approximate G_{η_ε} by $G_{\sqrt{\rho_{\mathrm{TF}}}} = G_\varepsilon$ and I_{η_ε} by $I_{\sqrt{\rho_{\mathrm{TF}}}} = I_\varepsilon$.

Assuming that the solution u_ε has a vortex line along γ, that is u_ε vanishes along γ with a winding number equal to 1, our aim is to estimate the energy of u_ε depending on γ. Our approximations rely on the fact that the ellipticity of the cross-section is weak and that ε is sufficiently small. We refer to [22] for details.

2.3. Estimate of $G_\varepsilon(v_\varepsilon)$

We want to estimate

$$G_\varepsilon(v_\varepsilon) = \int_{\mathcal{D}} \frac{1}{2}\rho_{\mathrm{TF}}|\nabla v_\varepsilon|^2 + \frac{\rho_{\mathrm{TF}}^2}{4\varepsilon^2}\big(1-|v_\varepsilon|^2\big)^2.$$

The mathematical techniques to approximate G_ε have been introduced in [28] in dimension 2 and in [29] in dimension 3, when ε is very small.

We expect that the vortex core is of size $\lambda\varepsilon$, where λ is a matching parameter. In the vortex core, the profile of v_ε is given by the cubic NLS equation and the energy at leading order produces a term in $\log(\lambda\rho_{\mathrm{TF}})$. Outside the vortex core, that is away from a tube of size $\lambda\varepsilon$, $|v_\varepsilon|$ is very close to 1 and only the phase of v_ε is of influence. The computation of the energy in that region uses the analogy with fluid vortices and we introduce the equivalent of a stream function that approximately solves a Bessel type equation. The computation is inspired by [30]. Finally, we determine the matching parameter λ and we find that each vortex line γ provides a contribution

$$G_\varepsilon(v_\varepsilon) \simeq \pi|\log\varepsilon| \int_\gamma \rho_{\mathrm{TF}}\,\mathrm{d}l \tag{12}$$

and we can also compute the interaction term in case of several vortices.

2.4. Estimate of $I_\varepsilon(v_\varepsilon)$

The estimate for I_ε is rather simple to get. Recall that the unique solution of (8) satisfies $\rho_{\mathrm{TF}}(\nabla S_\varepsilon - \Omega\times\mathbf{r}) = \Omega\,\mathrm{curl}\,\Xi_\varepsilon$. Hence we integrate by part in the expression for $I_{\eta_\varepsilon}(v_\varepsilon)$ to get

$$I_{\eta_\varepsilon}(v_\varepsilon) = \Omega\int_{\mathcal{D}} \Xi_\varepsilon\cdot\mathrm{curl}(\mathrm{i}v_\varepsilon,\nabla v_\varepsilon).$$

Let ϕ_ε be the phase of v_ε. Since v_ε is tending to one everywhere except on the vortex line, then $(\mathrm{i}v_\varepsilon,\nabla v_\varepsilon)\sim\nabla\phi_\varepsilon$, hence we can approximate $\mathrm{curl}(\mathrm{i}v_\varepsilon,\nabla v_\varepsilon)$ by $2\pi\delta_\gamma$. We use the value of Ξ and the fact that $\dot\gamma(t)\cdot\mathbf{e}_z = \mathrm{d}z$, to obtain

$$I_\varepsilon(v_\varepsilon) \simeq -\frac{\Omega\pi}{1+\alpha^2}\int_\gamma \rho_{\mathrm{TF}}^2\,\mathrm{d}z. \tag{13}$$

2.5. Final estimate for the energy

We use Eqs. (11)–(13) to derive the energy of a solution with a vortex line. The energy of any solution minus the energy of a solution without vortex is roughly the vortex contribution in the sense $E_\varepsilon(u_\varepsilon) - E_\varepsilon(\eta_\varepsilon)\simeq E[\gamma]$. We find that the vortex contribution is

$$E[\gamma] = \pi|\log\varepsilon|\int_\gamma \rho_{\mathrm{TF}}\,\mathrm{d}l - \frac{\Omega\pi}{(1+\alpha^2)}\int_\gamma \rho_{\mathrm{TF}}^2\,\mathrm{d}z. \tag{14}$$

The energy $E[\gamma]$ reflects the competition between the vortex energy due to its length (1st term) and the rotation term. Note that the rotation term is an oriented integral ($\mathrm{d}z$ not $\mathrm{d}l$), which actually forces the vortex to be along the z-axis, while the other term wants to minimize the length. This is why, according to the geometry of the trap, the shape of the vortex varies.

Let us point out that Svidzinsky and Fetter [30] have studied the dynamics of a vortex line depending on its curvature. For a vortex velocity equal to 0, the equation obtained in [30] is the same as the equation corresponding to the minimum of our approximate energy, though the formulation in [30] was not derived from energy considerations. Following our work, [18] have also derived an approximate expression for the energy. Note that the energy that we actually derive in [22] is slightly more involved than (14). In the regime of the experiments, it is reasonable to restrict to this expression (14), taking into account the fact that the vortex core is sufficiently small (it is of size ε in our units) and neglecting the interaction of the curve with itself. We are interested only in the presence of the first vortex. When there are several vortices, the energy has an extra term due to the repulsion between the lines $I(\gamma_i,\gamma_k)$:

$$E_\varepsilon(u_\varepsilon) - E_\varepsilon(\eta_\varepsilon) \simeq \sum_i E[\gamma_i] + \sum_{i\neq k} I(\gamma_i,\gamma_k), \tag{15}$$

where

$$I(\gamma_i,\gamma_k)=\pi\int_{\gamma_i}\rho_{\mathrm{TF}}\log\bigl(\mathrm{dist}(x,\gamma_k)\bigr)\,\mathrm{d}l.$$

A rigorous mathematical derivation of $E[\gamma]$ using Γ convergence has been performed in [31].

3. Single vortex line, study of $E[\gamma]$

The analysis described in this section relies on [23,24]. From now on, we will define

$$\overline{\Omega}=\frac{\Omega}{(1+\alpha^2)|\log\varepsilon|}.$$

The energy of the vortex free solution is zero. Thus, a vortex line is energetically favorable when Ω,β are such that $\inf_\gamma E[\gamma]<0$. Recall that β determines the elongation of the trap and is included in the expression of ρ_{TF}. Our aim is to study the shape of the vortex lines γ minimizing $E[\gamma]$. Taking the straight vortex γ_s as a test function in $E[\gamma]$, allows us to compute the critical angular velocity Ω_1 for which a straight vortex has a lower energy than a vortex free solution. At $\Omega=\Omega_1$, $E[\gamma_s]=0$, so that we find $\Omega_1=(5/4)(1+\alpha^2)|\log\varepsilon|$. We have checked numerically that there is a range of value of Ω less than Ω_1 for which a bent vortex has a negative energy, in particular a lower energy than a straight vortex and the vortex free solution. We are going to check this analytically here by looking at the stability and instability of the straight vortex and prove that when the condensate has a cigar shape the first vortex is bent, while when it is a pancake, the first vortex is straight and lies on the axis of rotation.

First of all, it has been observed numerically [17] that the vortex line lies in the plane closest to the axis of rotation and we can provide a rigorous justification:

Theorem 3.1. *If $\alpha\geqslant 1$, then the energy $E[\gamma]$ is minimized when the vortex line lies in the (y,z) plane, that is the plane closest to the axis.*

Indeed, if we have a curve γ parametrized as $\gamma(t)=(x(t),y(t),z(t))$, then we can define the new curve $\tilde\gamma(t)=(0,\tilde y(t),\tilde z(t))$ by $\tilde z(t)=z(t)$ and $\tilde y(t)=\sqrt{x^2/\alpha^2+y^2}$. Then $\rho_{\mathrm{TF}}(\gamma(t))=\rho_{\mathrm{TF}}(\tilde\gamma(t))$. Since $\alpha\geqslant 1$, $\dot{\tilde y}^2\leqslant\dot x^2+\dot y^2$, hence $\rho_{\mathrm{TF}}(\tilde\gamma)|\dot{\tilde\gamma}|-\overline{\Omega}\rho_{\mathrm{TF}}(\tilde\gamma)\dot{\tilde z}\leqslant\rho_{\mathrm{TF}}(\gamma)|\dot\gamma|-\overline{\Omega}\rho_{\mathrm{TF}}(\gamma)\dot z$. It follows that the energy of the new curve $E[\tilde\gamma]$ is less or equal than $E[\gamma]$. If $\alpha=1$, that is the cross section is a disc, then our arguments imply that the vortex line is planar, but of course all transversal planes are equivalent.

From now on, we will assume that the curve lies in the plane (y,z), so that $x=0$ and we denote by ρ, the value of ρ_{TF} that only depends on y and z. For every Ω, there exists a minimizer of $E[\gamma]$. Any minimizer is either the vortex free state, or has a vortex along the z-axis or is supported in the set $\{y>0\}$ and is bounded away from the z-axis. If $\Omega\rho_0<1/2$, we can prove that there cannot exist a critical point of the energy which lies in the half yz plane $y>0$. See [24].

Let us investigate the existence of a bent vortex. Notice from the expression of E, that for $E[\gamma]$ to be negative, we need $\rho-\overline{\Omega}\rho^2$ to be negative somewhere, that is $\overline{\Omega}\rho>1$. For fixed $\overline{\Omega}$, we define the regions

$$\mathcal{D}_i:=\bigl\{(y,z):\overline{\Omega}\rho(y,z)>1\bigr\},\qquad \mathcal{D}_o:=\mathcal{D}\setminus\mathcal{D}_i. \tag{16}$$

We will refer to these sets as 'the inner region' $\mathcal{D}_i$ and 'the outer region' $\mathcal{D}_o$ respectively. In the outer region, the energy of a vortex per unit arc length is necessarily positive, since $\rho-\overline{\Omega}\rho^2>0$, whereas in the inner region, for appropriately oriented vortices it can be negative since $\rho-\overline{\Omega}\rho^2<0$. One can see easily that for γ to have a negative energy, part of the vortex line has to lie in the inner region, that is close to the center of the cloud. Note that for $\mathcal{D}_i$ to be nonempty, we need at least $\overline{\Omega}\rho_0>1$. This, with the fact that $\overline{\Omega}_1\rho_0=5/4$, indicates that the critical velocity Ω_c for the existence of a vortex is such that

$$\bigl(1+\alpha^2\bigr)|\log\varepsilon|<\Omega_c\leqslant\frac{5}{4}\bigl(1+\alpha^2\bigr)|\log\varepsilon|.$$

In the region $\mathcal{D}_i$, we will see that the vortex is close to the axis for all β. On the other hand, in the region $\mathcal{D}_o$, the vortex goes to the boundary along the quickest path: if β is small, perpendicularly to the boundary, which gives rise to a bent vortex and if $\beta>1$, the vortex stays along the axis of rotation. In [23], we prove the following

Proposition 3.2. *For all β and all Ω, in the inner region $\mathcal{D}_i$, the straight vortex minimizes the energy restricted to $\mathcal{D}_i$.*

Proposition 3.3. *For $\beta\geqslant 1$, in the outer region $\mathcal{D}_o$,the straight vortex minimizes the energy restricted to $\mathcal{D}_o$.*

Note that in the outer region, Proposition 3.3 only holds for $\beta > 1$. If $\beta < 1$, the situation is somewhat more complicated: $\int_{\gamma_o} \rho \, dl$ is minimized by a path that joins $\mathcal{D}_i$ to $\partial\mathcal{D}$ along the y-axis, whereas $-\int_{\gamma_o} \rho^2 \, dz$ is minimized by the straight vortex running along the z-axis. The minimizer of the full energy reflects the competition between these two terms, and hence is bent. In particular, as a corollary of the above propositions we deduce

Theorem 3.4. *For $\beta \geqslant 1$, $E[\gamma] \geqslant \inf(0, E[\gamma_s])$, where γ_s is the straight vortex along the z-axis. If $E[\gamma_s] < 0$, the equality can happen only if γ is the straight vortex.*

Note that for each z, there is a critical velocity $\Omega_{2d}(z)$ for the existence of a vortex in the 2-dimensional section where z is constant. The region $\mathcal{D}_i$ corresponds to points z such that $\Omega > \Omega_{2d}(z)$. We now investigate further on the stability of the straight vortex. Writing a Taylor series expansion for E, one finds that $E[\gamma_\delta] = E[\gamma_s] + \frac{\delta^2}{2}(v, E''[\gamma_s]v) + O(\delta^3)$. We say that the straight vortex is stable if $(v, E''[\gamma_s]v) > 0$ for all v, and unstable if $(v, E''[\gamma_s]v) < 0$ for some v.

Theorem 3.5. *The straight vortex is stable if*

$$\overline{\Omega}\rho_0 > \frac{3}{4} + \frac{1}{4\beta^2}. \tag{17}$$

The straight vortex is unstable if $\beta < 1/\sqrt{3}$ and

$$\overline{\Omega}\rho_0 < \frac{1}{6} + \frac{1}{6\beta^2}. \tag{18}$$

Note that the 2 values are consistent in the sense that they both scale like $1/\beta^2$ when β is small. For $\overline{\Omega}$ large, one expects several vortices in the condensate, but the fact that a straight vortex is stable gives an indication that for $\overline{\Omega}$ large, each vortex should be nearly straight, which is consistent with the observations [16]. Recall that the stabilization of the cloud requires that the rotation is not stronger than the trapping potential, which reads in our notations $\overline{\Omega} < 1/\varepsilon$.

Remark 1. It is interesting to see what happens in Theorem 3.5 when $\overline{\Omega}\rho_0 = 5/4$, that is when the straight vortex has zero energy. The first inequality yields that if $\beta > 1/\sqrt{2}$, then the straight vortex is stable for all $\overline{\Omega}$ such that $\overline{\Omega}\rho_0 > 5/4$, that is when $E[\gamma_s] < 0$. If $\beta > 1$, we have seen that γ_s is not just stable but in fact minimizes E. The second inequality implies that, if $\beta < \sqrt{2/13} \approx 0.39$ then the straight vortex is unstable at the velocity $\overline{\Omega}\rho_0 = 5/4$ at which $E[\gamma_s] = 0$. As a result, for these values of β, the first vortex to nucleate as $\overline{\Omega}$ increases is a bent vortex. Note that it has been observed in [30] that for $\beta \lesssim 1/2$, the ground state of the system exhibits a bent vortex. Numerical results of [17] also show that bent vortices are energetically favorable when β is small.

All this indicates that by varying the elongation of the condensate, one may hope to go from a situation where the first vortex is bent, to a situation where it is straight.

4. Numerical simulations

In this section, we show numerical simulations of solutions of the full Gross–Pitaevskii equations that illustrate the properties described above. The computations published in this part are published in [25]. We compute critical points of $E(u)$ by solving the norm-preserving imaginary time propagation of the corresponding equation:

$$\frac{\partial u}{\partial t} - \frac{1}{2}\nabla^2 u + i(\Omega \times \mathbf{r}) \cdot \nabla u = \frac{1}{2\varepsilon^2} u\left(\rho_{\mathrm{TF}} - |u|^2\right) + \mu_\varepsilon u, \tag{19}$$

with $u = 0$ on $\partial\mathcal{D}$ and μ_ε the Lagrange multiplier for the constraint $\int_{\mathcal{D}} |u|^2 = 1$. A hybrid 3 steps Runge–Kutta–Crank–Nicolson scheme is used to march in time. We use various initial data, without vortices or with vortices on the z-axis or off the axis.

We have observed three different types of single vortex configurations as shown in Fig. 1: planar U vortices, planar S vortices and non-planar S vortices. The U vortices are the bent vortices computed in [17,18] and theoretically studied in [22,23]. They are global minimizers of the energy. The S configurations were observed experimentally very recently [14] and are only local minimizers of the energy.

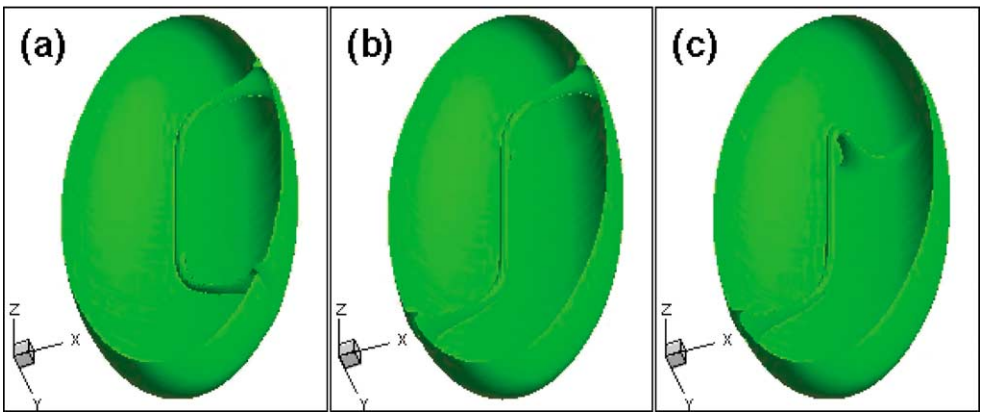

Fig. 1. Single vortex configurations in BEC: (a) U vortex; (b) planar S vortex; (c) non-planar S vortex. Isosurfaces of lowest density within the condensate.

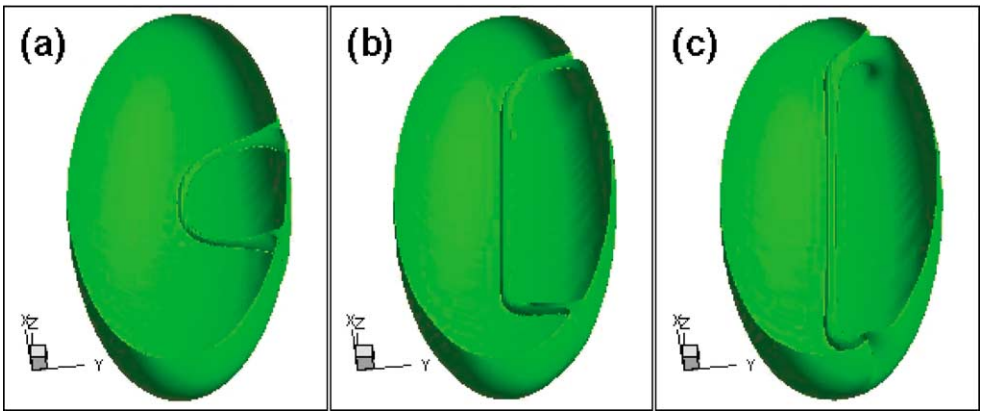

Fig. 2. Single U vortex configurations for: (a) $\widetilde{\Omega}/\omega_x = 0.42$; (b) $\widetilde{\Omega}/\omega_x = 0.58$; (c) $\widetilde{\Omega}/\omega_x = 0.78$.

4.1. U vortex

The U vortex is a planar vortex formed of 2 parts: the central part is a line which stays on the z-axis and the outer part reaches the boundary of the condensate perpendicularly. When Ω increases, the central straight part gets longer (Fig. 2) and the angular momentum (L_z) increases to 1 (Fig. 3).

The U vortex lies either in the x–z or y–z plane. Starting with an initial condition which is not in one of these plane yields a final state in the y–z plane, which is the plane closest to the z axis.

The shape of the the U vortex and its preferred location in the y–z plane can be analyzed using the approximate energy $E[\gamma]$: if γ is not in the x–z or y–z plane, then one can construct small perturbations of γ that preserve ρ_{TF} and lower the energy. This implies that γ cannot be a critical point of the energy because the gradient is not zero. Of course, if the ellipticity of the cross-section is small, the gradient is small, which may allow to observe these configurations.

In order to understand the existence of the straight central part of the U vortex, one can also refer to the analysis described above with the inner and outer region (16). In the region $\mathcal{D}_i$, the vortex is straight and in $\mathcal{D}_o$, it is bending.

Fig. 3 shows the energy and angular momentum variation with $\widetilde{\Omega}$ for the single vortex configurations. The U vortices exist only for $\widetilde{\Omega}$ bigger than a critical value $\Omega_0 = 0.42\omega_x$. It is interesting to note that at Ω_0, the energy of the U vortex is bigger than the energy of the vortex free solution (we have set to zero the energy of the vortex free solution). A zoom in this region shows that Ω_0 is very close to the angular velocity Ω_c for which the energy of the vortex free solution is equal to the energy of the U vortex.

Fig. 3 also shows that the angular momentum L_z of the U vortex for $\Omega = \Omega_0$ does not go to 0. This suggests that in fact there could be another U solution for $\Omega > \Omega_0$. Using an ansatz, another type of U solution is obtained in [18] which is a saddle

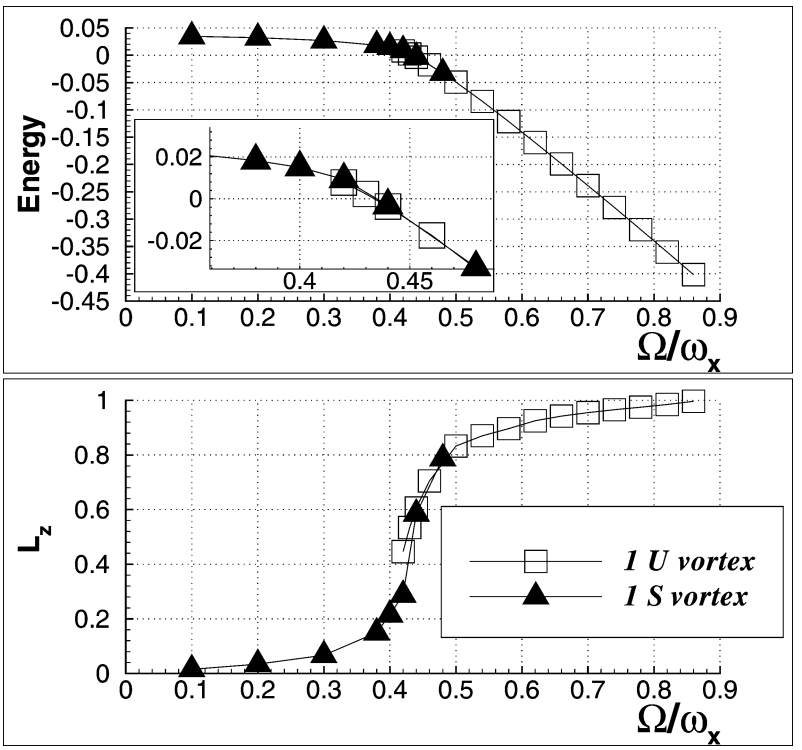

Fig. 3. Energy (in units of $\hbar\omega_x$) and angular momentum per particle (in units of $\hbar$) for the single vortex configurations.

point of the energy: it is away from the axis and has lower angular momentum. In [23], it is proved rigorously that for Ω small, there is no U as a critical point of the energy.

4.2. S vortex

Motivated by the experiments of [14], we compute new critical points of the energy, which are S configurations (see Fig. 1). Several numerical experiments were performed, starting from different initial conditions containing an ansatz for the S vortex.

The planar S can be regarded as a U, with the half-part in the plane $z < 0$ rotated with respect to the z-axis by 180 degrees. The nonplanar S are such that the projections of the branches on the x–y plane are orthogonal, i.e., the rotation of the branches is of 90 degrees. We could check that nonplanar S configurations with an angle between the branches different from 90 degrees do not exist.

The S vortices exist for all values of Ω while the U only exist for $\Omega > \Omega_0$. When Ω decreases, the extension of the S along the z-axis goes downwards as shown in Fig. 4, the angular momentum decreases to 0 (Fig. 3) and the vortex tends to the horizontal axis. Note that a vortex along the horizontal axis has $L_z = 0$, but a positive energy. On the other side, when Ω increases, the S gets straighter and it tends to the vertical axis.

S vortices are critical points of $E[\gamma]$ for any Ω, but never minimizers of $E[\gamma]$. The difference in energy (and angular momentum) between U and S vortices is very small, as illustrated in Fig. 3 because an S vortex is almost like a U with a half-part rotated by 180 degrees.

As already mentioned for the U vortex, stable planar S configurations lie either in the x–z or y–z plane. As for the U, this can be explained using the limiting energy $E[\gamma]$ and considering separately the upper or lower part of the S. As soon as the cross section is not a disc, if the upper or lower branch of the S configuration does not lie in the x–z or y–z plane, then the gradient of the vortex line energy can never be zero when γ is varied. This is why the only possible 3D S configuration is when the upper and lower branches of the S are perpendicular.

4.3. Minimizer with fixed L

The energy E_ε or $E[\gamma]$ can be split into 2 terms H and L_z, such that $E = H - \Omega L_z$. As pointed out in [14], the minimization problem which is related to the experiments, is rather to minimize H, while fixing L_z, rather than minimizing $H - \Omega L_z$. This

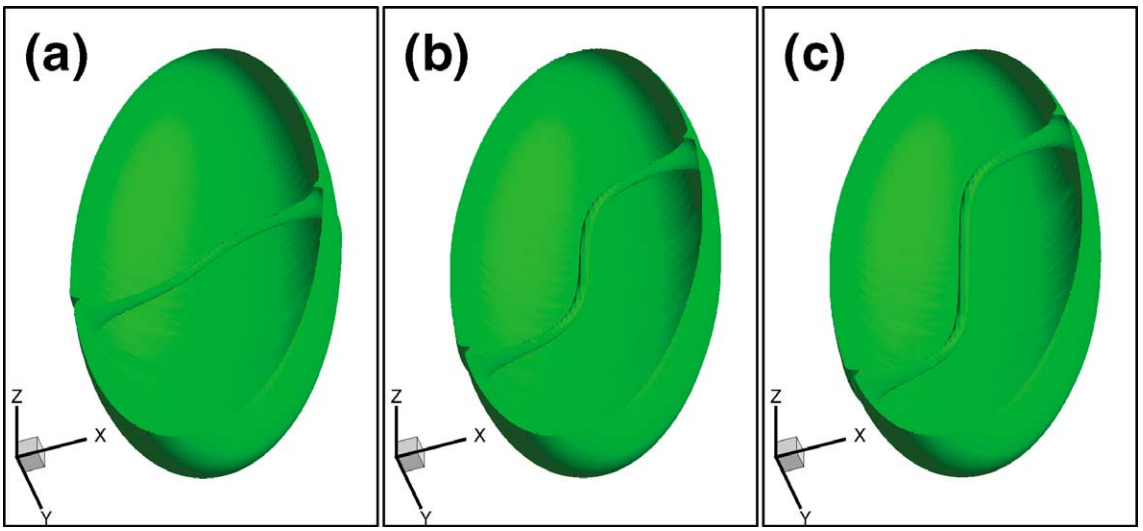

Fig. 4. Single S vortex configuration for: (a) $\Omega/\omega_x = 0.38$; (b) $\Omega/\omega_x = 0.44$; (c) $\Omega/\omega_x = 0.48$.

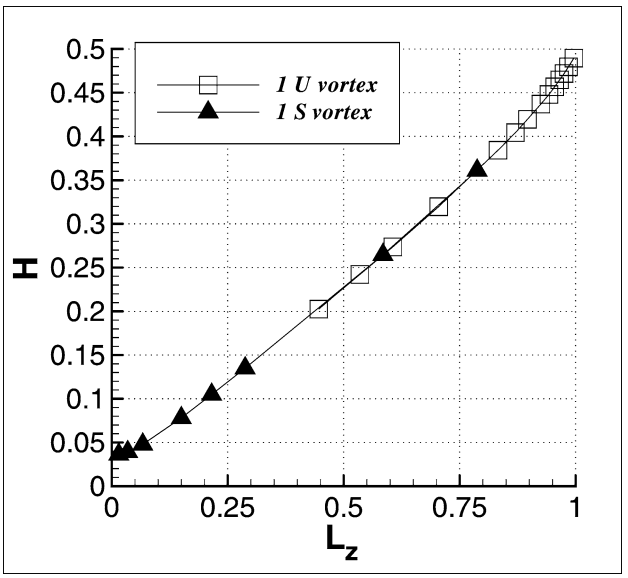

Fig. 5. H versus L_z for single vortex configuration.

has been studied in the 2-dimensional setting in [1], but the numerical simulation in 3D is still an open problem. One can notice that if a given configuration with $H = h$ and $L_z = l$ minimizes $E = H - \Omega L_z$ for some Ω, then h minimizes H under the constraint that $L_z = l$: indeed if $H' = H(u)$ with $L_z(u) = l$, then $H' - \Omega l \geqslant h - \Omega l$, since (h, l) minimizes E, and this implies that $H' \geqslant h$. Moreover Ω is the slope to the curve $H(L_z)$ at the point (h, l) and the property of minimizing E that is for all h', l',

$$h' - \Omega l' \geqslant h - \Omega l \tag{20}$$

implies that the curve $H(L_z)$ lies above its tangent at this point.

We have plotted H as a function of L_z (Fig. 5). We can check that the curve is convex, and above its tangent, which is consistent with the fact that we have computed minimizers of the energy.

We know that the U solution exists for $\Omega \geqslant \Omega_0$ and has $L_z > 0.4$. For $L_z < 0.4$, we expect that the process of minimizing H with fixed L_z would produce U vortices and the curve $H(L_z)$ should be concave in this region, but we have not been able to

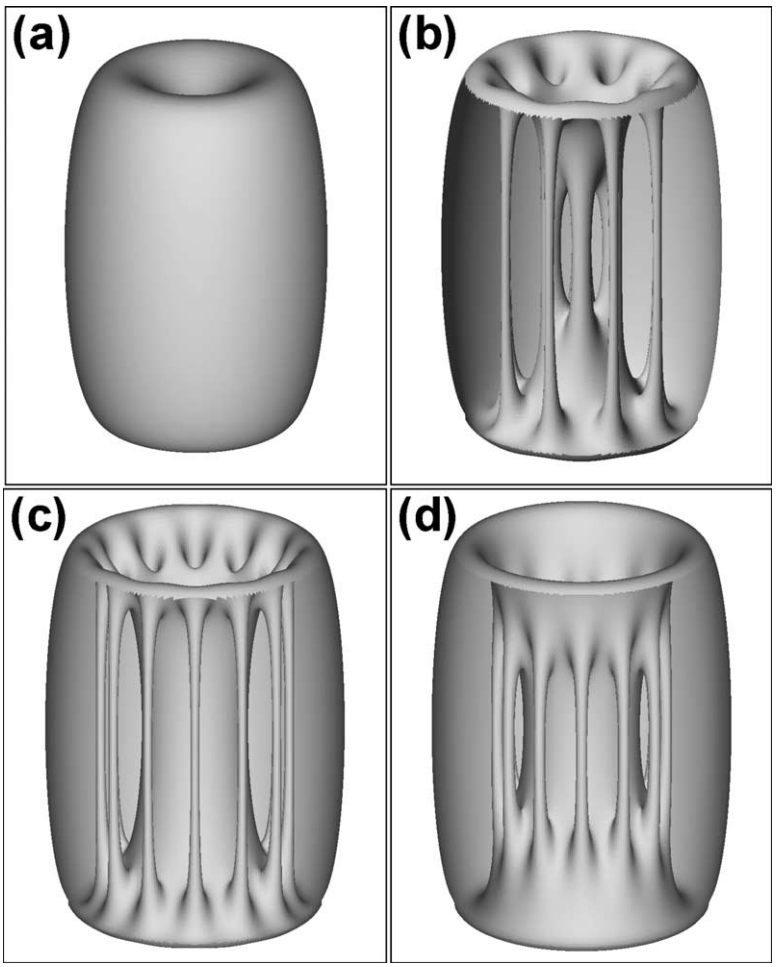

Fig. 6. ($\alpha = 1.1$) Side view of the condensate for: (a) $\Omega/\omega_\perp = 0.12$; (b) $\Omega/\omega_\perp = 0.2$; (c) $\Omega/\omega_\perp = 0.28$;, (d) $\Omega/\omega_\perp = 0.32$. Isosurface of lowest density.

perform the simulation. In [23], we have proved that for L_z close to 0, $H \geqslant C L_z^{2/3}$, which is a first indication to the concavity of the curve.

4.4. Other simulations

In [25], we have also computed configurations with several vortices. More recent simulations [32] take into account other types of traps than the harmonic trap and allow us to see giant vortices. Following recent experiments at the ENS [33] where a blue detuned laser beam is superimposed to the magnetic trap holding the atoms, we replace the harmonic trapping potential by a combined harmonic and quartic term: ρ_{TF} is replaced by $(1-a)r^2 + kr^4 + \beta^2 z^2$. As Ω increases, the vortex lattice evolves into a vortex lattice with hole, as shown in Fig. 6.

5. Vortex shedding in the Painlevé boundary layer of a Bose–Einstein condensate

Raman et al. [29] have found experimental evidence for a critical velocity under which there is no dissipation when a detuned laser beam is moved in a Bose–Einstein condensate. This critical velocity has been related to the one found by Frisch et al. [34] for the problem of a 2D superfluid flow around an obstacle in the framework of Nonlinear Schrodinger Equation: below a critical velocity, the flow is stationary and dissipationless, while beyond this critical velocity, the flow becomes time dependent and vortices are emitted. Numerical simulations have been done for this type of problem in 2D [35] and 3D [36].

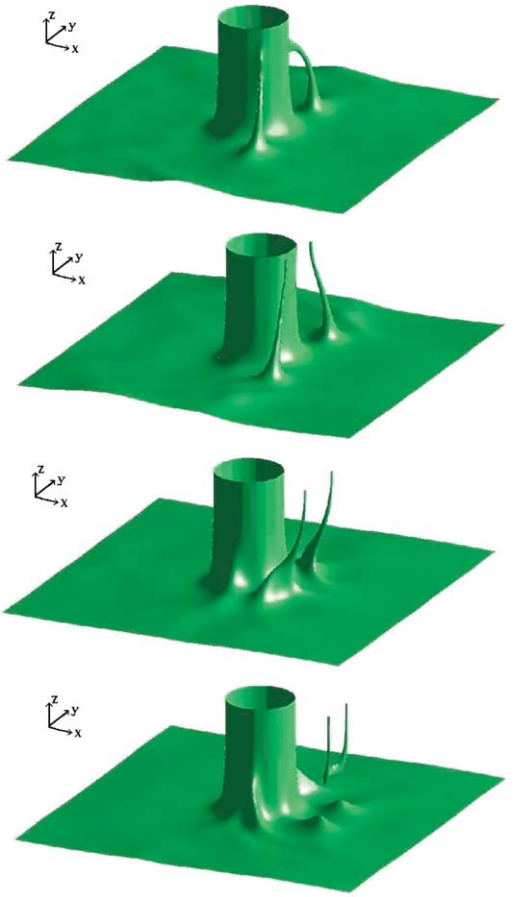

Fig. 7. A sequence of isosurface snapshots of $|u|$ for $v = 0.28$: (a) formation of vortex handles $t = 0.04$; (b) detachment from obstacle $t = 0.08$; (c) bending of vortex tubes $t = 0.12$; and (d) formation of vortex *half* rings $t = 0.16$.

In [26], we want to take into account the 3D geometry of the experiment of [11–13]. Our aim is to understand the mechanism of vortex nucleation in the boundary region. We analyze the origin of this critical velocity in the low density region close to the boundary layer of the cloud. In the frame of the laser beam, we do a blow up on this low density region which can be described by a Painlevé equation and write the approximate equation satisfied by the wave function in this region. We find that there is always a drag around the laser beam. Though the beam passes through the surface of the cloud and the sound velocity is small in the Painlevé boundary layer, the shedding of vortices starts only when a threshold velocity is reached. At low velocity, there is a stationary solution without vortex and the drag is small. The drag is not a consequence of the shedding of vortices, and finally of a time dependent density and velocity field. The origin of this drag is in the radiation condition for the wavefield: the motion changes continuously the structure of the solution seen in the frame of reference of the 'fluid' at infinity. The drag increases smoothly as the velocity increases. We study the transition toward a time dependent regime of vortex shedding, which happens at a critical velocity. The critical velocity that we find is lower than the 2D critical velocity at the center of the cloud coming from the computation of [34]. Vortices are nucleated close to the boundary of the cloud and the tubes grow and detach to form rings that move downstream (see Fig. 7). When tubes are emitted, significantly large drag values are observed.

References

[1] D. Butts, D. Rokhsar, Nature 397 (1999) 327.
[2] F. Dalfovo, S. Giorgini, L. Pitaevskii, S. Stringari, Rev. Mod. Phys. 71 (1999) 463.
[3] D.L. Feder, C.W. Clark, B.I. Schneider, Phys. Rev. Lett. 82 (1999) 4956.
[4] M.R. Matthews, et al., Phys. Rev. Lett. 83 (1999) 2498.
[5] D.L. Feder, C.W. Clark, B.I. Schneider, Phys. Rev. A 61 (1999) 011601(R).

[6] Y. Castin, R. Dum, Eur. Phys. J. D 7 (1999) 399.
[7] K. Madison, F. Chevy, V. Bretin, J. Dalibard, Phys. Rev. Lett. 84 (2000) 806.
[8] K. Madison, F. Chevy, W. Wohlleben, J. Dalibard, J. Mod. Opt. 47 (2000) 2715.
[9] A.A. Svidzinsky, A.L. Fetter, Phys. Rev. Lett. 84 (2000) 5919.
[10] A.L. Fetter, A.A. Svidzinsky, cond-mat/0102003.
[11] C. Raman, M. Köhl, R. Onofrio, D.S. Durfee, C.E. Kuklewicz, Z. Hadzibabic, W. Ketterle, Phys. Rev. Lett. 83 (1999) 2502–2505.
[12] R. Onofrio, C. Raman, J.M. Vogels, J.R. Abo-Shaeer, A.P. Chikkatur, W. Ketterle, Phys. Rev. Lett. 85 (2000) 2228–2231.
[13] C. Raman, R. Onofrio, J.M. Vogels, J.R. Abo-Shaeer, W. Ketterle, J. Low Temp. Phys. 122 (2001) 99–116.
[14] P. Rosenbuch, V. Bretin, J. Dalibard, Phys. Rev. Lett. 89 (2002) 200403.
[15] C. Raman, J.R. Abo-Shaeer, J.M. Vogels, K. Xu, W. Ketterle, Phys. Rev. Lett. 87 (2001) 210402.
[16] J.R. Abo-Shaeer, C. Raman, J.M. Vogels, W. Ketterle, Science 292 (2001) 476.
[17] J.J. García-Ripoll, V.M. Perez-García, Phys. Rev. A 63 (2001) 041603(R);
J.J. García-Ripoll, V.M. Perez-García, Phys. Rev. A 64 (2001) 053611.
[18] M. Modugno, L. Pricoupenko, Y. Castin, Eur. Phys. J. D 22 (2003) 235–257.
[19] F. Dalfovo, L. Pitaevskii, S. Stringari, Phys. Rev. A 54 (1996) 4213.
[20] A.L. Fetter, D.L. Feder, Phys. Rev. A 58 (1998) 3185.
[21] A. Aftalion, Q. Du, Phys. Rev. A 64 (2001) 063603.
[22] A. Aftalion, T. Riviere, Phys. Rev. A 64 (2001) 043611.
[23] A. Aftalion, R.L. Jerrard, Phys. Rev. A 66 (2002) 023611.
[24] A. Aftalion, R.L. Jerrard, C. R. Acad. Sci. Paris, Ser. I 336 (2003).
[25] A. Aftalion, I. Danaila, Phys. Rev. A. 68 (2003) 023603.
[26] A. Aftalion, Q. Du, Y. Pomeau, Phys. Rev. Lett. 91 (2003) 090407.
[27] L. Lassoued, P. Mironescu, J. Anal. Math. 77 (1999) 1.
[28] F. Bethuel, H. Brezis, F. Helein, Ginzburg–Landau Vortices, Birkhäuser, 1994.
[29] T. Riviere, COCV 1 (1996) 77.
[30] A.A. Svidzinsky, A.L. Fetter, Phys. Rev. A 62 (2000) 63617.
[31] R.L. Jerrard, Preprint.
[32] A. Aftalion, I. Danaila, cond-mat/0309668.
[33] V. Bretin, S. Stock, Y. Seurin, J. Dalibard, cond-mat/0307464.
[34] T. Frisch, Y. Pomeau, S. Rica, Phys. Rev. Lett. 69 (1992) 1644.
[35] C. Huepe, M.E. Brachet, Physica D 144 (2000) 20–36.
[36] B. Jackson, J.F. McCann, C.S. Adams, Phys. Rev. A 61 (2000) 051603.